

In-vivo measurements of axon density and axon diameter in the Corpus Callosum in Multiple Sclerosis

Torben Schneider¹, Wallace Brownlee¹, Jonathan Clayden², Olga Ciccarelli³, David H Miller¹, Daniel C Alexander⁴, and Claudia A M Wheeler-Kingshott¹
¹NMR Research Unit, Department of Neuroinflammation, Queen Square MS Centre, UCL Institute of Neurology, London, United Kingdom, ²UCL Institute of Child Health, Imaging & Biophysics Unit, London, United Kingdom, ³Brain Repair & Rehabilitation, UCL Institute of Neurology, London, United Kingdom, ⁴Centre of Medical Image Computing, Department of Computer Science, University College London, London, United Kingdom

Purpose: To apply a novel diffusion weighted imaging (DWI) protocol that achieves high-resolution *in-vivo* axon diameter and density estimates in the corpus callosum (CC) of subjects with Multiple Sclerosis (MS) and healthy controls (HC). While previous studies have reported white matter atrophy¹ and DTI changes² in CC, these parameters are not specific to the microscopic damage associated with the disease. In the last few years, advances in DWI modeling^{3,4} and sequence optimization⁴⁻⁶ have enabled microstructure-specific measures of axon diameter and axon density *in-vivo* and at routine clinical gradient strengths of around 60mT/m. These novel measures open new possibilities to study the microstructural damage associated with neurodegenerative diseases. Here, we propose to measure axon diameter and density in the CC of 5 MS patients and compare with 5 age- and gender-matched HC. We employ a previously published analysis pipeline, which combines advanced computational DWI modelling with an optimised protocol for fast *in-vivo* DWI.

Methods: *Subjects:* Five MS patients (mean age 39 +/- 9 years, median EDSS score 4, 3 female) and 5 age and sex-matched HC. *MR acquisition:* Scanning was performed on a 3T Philips Achieva system with a 32-channel head coil, using the following sequences (i) multi-echo PD/T2 sequence for lesion identification: voxel size 1x1x3mm³, FOV=240x240mm², 50 slices, TE=19/88ms, TR=3500, SENSE=1.7 (ii) Optimised DWI protocol (as previously described⁶): 10 sagittal slices with high in-plane resolution and centered on the mid-sagittal plane of the CC, perpendicular to the dominant fibre direction of the CC. The protocol was derived from a computational optimization and contained 6 different combinations of diffusion time, diffusion encoding length and b-value: one acquisition parallel to the CC fibres and 5 others perpendicular to them, plus one additional DTI-type acquisition for a total of 108 DWI images (see reference 6 for full protocol). Other acquisition parameters were: voxel size: 1x1x4mm³, FOV=96x96mm², TR=6000ms, 2 averages, using an outer-volume suppressed ZOOM acquisition [X] to avoid fold-over artifacts. DWI data was corrected for motion and eddy current distortions using the eddy tool of FSL5 and NiftyReg⁷. *Model fitting:* We fitted a single axon diameter model⁴, based on the minimal model of white matter diffusion (zeppelin-cylinder-ball in the compartment model taxonomy⁸) with an additional T2 relaxation factor. The fitted model parameters were: volume fractions of intra-axonal and CSF compartments (f_{ax} , f_{csf}), axon diameter index (d), net magnetization $M_{TE=0}$ and T2. We fixed the intra-axonal and CSF diffusivity values to physiologically plausible values ($D_{ax}=2\text{MUm}^2/\text{s}$, $D_{CSF}=3\text{MUm}^2/\text{s}$). The free model parameters were fitted by running MCMC (samples: 100; steps: 50; burn-in: 5000) and taking the mean of each parameter's posterior distribution. All analysis was performed in Camino¹⁰ and TractoR¹¹. *ROI analysis:* In each subject, the CC was manually segmented in three mid-sagittal slices. We excluded voxels that either had low FA<0.5 or had fibre directions considered to be too co-linear with respect to the perpendicular gradient vectors (<65 degree). From the CC masks, the AP median line was computed and used to divide the CC in anterior, middle and posterior ROIs with equivalent extent in AP direction (see Figure 1). In the MS subjects, we also manually delineated any visible lesions on the DWI b=0 (TE=58ms) that were visually confirmed on the PD/T2 images. We pooled all voxel-wise model parameters from each ROI to generate boxplots for healthy white matter in HC and normal appearing white matter (NAWM = CC ROIs without lesion) and lesions in MS.

Results and discussion: Figure 1 shows example maps of f_{csf} , f_{ax} and d in one HC and two MS subjects: one with no CC lesions and the other one with a lesion in the splenium. In the healthy subject we see the trend of low-high-low axon diameter index, as expected both from histology and previous studies. The d values of 6-12MUm are higher than expected from histology, but in agreement with previously reported values in HCs using a similar protocol⁶. The f_{ax} values are consistently high (between 0.5-0.7) over the whole CC, while f_{csf} suggests little to no presence of CSF outside the CC boundaries. Both MS1 and MS2 clearly exhibit similar amounts of extensive CC thinning. Differences between MS1 and MS2 emerge in the preserved CC WM. In MS1, d values resemble more the HC, while d is elevated (>10MUm) in MS2, particularly in the splenium lesion. In both MS1 and MS2, f_{ax} was markedly reduced in the middle and posterior part of the CC. The anterior f_{ax} values are more similar to HC. The f_{csf} is similar in the center of WM but overall is higher than in HC, signaling increased partial volume due to CC atrophy. Figure 2 shows boxplots of the f_{csf} , f_{ax} and d parameters obtained from all 10 subjects in the anterior, middle and posterior parts of healthy WM, NAWM and lesion masks (number of lesions: n=2 anterior; n=1 middle; n=2 posterior). The values in the HC ROIs support our observation in the exemplary HC case. We observe severe CC atrophy in all MS cases, which is reflected in the higher variation of all parameter estimates in the NAWM compared to HC, and also in increased f_{csf} values over the whole CC. We also see that f_{ax} decreases in mid and posterior NAWM, and further still in lesion tissue, compared to HC. While this, still, might be an effect of atrophy, the large differences between NAWM, lesion and HC are observed in the posterior part of the CC, which includes the splenium with a large number of pure WM voxels even in the MS cases. Therefore, the decrease in f_{ax} in NAWM and lesion can be related to axonal loss in the affected structures. Histology in MS suggests that axonal loss is associated with a loss of small fibres, while larger fibres are preserved¹². We observe an increase in axon diameter index in mid and posterior lesion tissue, but not in the anterior part. Unfortunately, the sample size here is too small to investigate whether this is simply due to patient-specific differences or whether it reflects regional differences in MS pathology. A preliminary power analysis (significance=5%, power=99%) suggest at least $n>18$ subjects per group to detect significant changes in f_{ax} between HC and MS, and $n>32$ between HC and NAWM. For d , $n>30$ is required to significantly distinguish HC and lesion tissue, and $n>269$ would be needed to distinguish HC and NAWM.

Conclusion: We have demonstrated estimates of axon diameter and density in the CC of MS patients and healthy controls using a standard clinical MRI. Our findings suggest loss of axonal tissue and fibre integrity in both NAWM and lesions in MS compared to HC, which is consistent with findings from previous studies using DTI² and other complementary MRI techniques¹³. This also follows results from histological assessment of MS specimen¹⁴. Furthermore we report regional increase of axon diameter index in posterior and mid parts of the CC, in agreement with reported preferential axonal loss reported *ex-vivo* MS spinal cord¹². Future work will investigate validation of these new imaging parameters with histology and will address the challenge of increasing spatial resolution, given the severe atrophy in MS CC. However, considering the small sample size, these results are encouraging and warrant studying them in a larger cohort and in different MS subgroups.

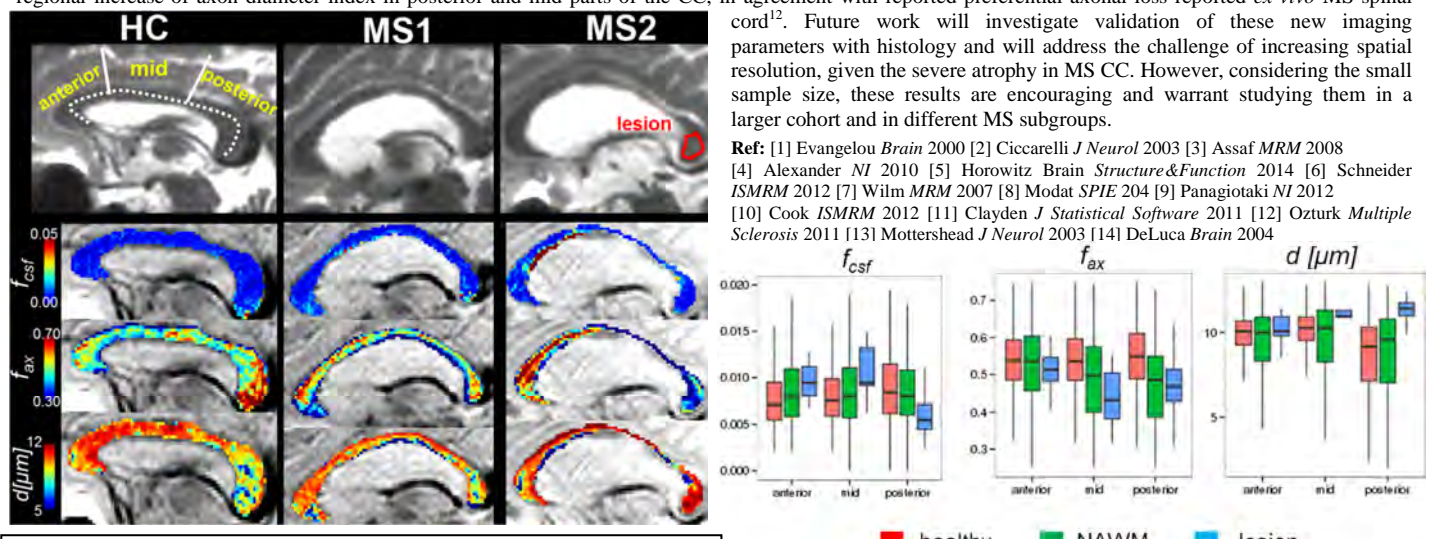


Figure 1: T2-weighted images of the CC (first row) and microstructure parameter maps in one healthy control (HC) and two MS subject (MS1 & MS2). Illustrations of the CC midline and CC parcellation are shown on the b=0 image of the HC. The lesion site in MS2 is marked in red.

Figure 2: Boxplots of model parameters pooled over all ROIs in HC and NAWM and lesion in MS subjects.

We thank the UK MS Society, Department of Health's NIHR BRC, EPSRC (EP/I027084/1) and ISRT for their support.